Astron. Astrophys. 351, 741–746 (1999)

ASTRONOMY AND ASTROPHYSICS

# Electron Firehose instability and acceleration of electrons in solar flares

**Gunnar Paesold**[1,2] **and Arnold O. Benz**[1]

[1] Institute of Astronomy, ETH-Zentrum, 8092 Zürich, Switzerland
[2] Paul Scherrer Institute, Würenlingen und Villigen, 5232 Villigen PSI, Switzerland

Received 9 September 1999 / Accepted 23 September 1999

**Abstract.** An electron distribution with a temperature anisotropy $T_\parallel/T_\perp > 1$ can lead to the Electron Firehose instability (Here $\parallel$ and $\perp$ denote directions relative to the background magnetic field $\mathbf{B}_0$). Since possible particle acceleration mechanisms in solar flares exhibit a preference of energizing particles in parallel direction, such an anisotropy is expected during the impulsive phase of a flare. The properties of the excited waves and the thresholds for instability are investigated by using linearized kinetic theory. These thresholds were connected to the pre-flare plasma parameters by assuming an acceleration model acting exclusively in parallel direction. For usually assumed pre-flare plasma conditions the electrons become unstable during the acceleration process and lefthand circularly polarized waves with frequencies of about $\sim |\Omega_p|$ are excited at parallel propagation. Indications have been found, that the largest growth rates occur at oblique propagation and the according frequencies lie well above the proton gyrofrequency.

**Key words:** acceleration of particles – instabilities – Sun: particle emission – Sun: X-rays, gamma rays – Sun: corona – Sun: flares

## 1. Introduction

Particle acceleration is a phenomenon occurring at many different sites throughout the universe. An important example of particle acceleration are solar flares, offering a wide range of observations that allow one to probe electron and ion acceleration. It is now widely accepted that the hard X-ray emission observed by various spacecraft reflects the energization of almost all electrons in the flaring plasma to energies up to $\sim 25\mathrm{keV}$. These observations and the observed magnetic fields encompassing the solar flare suggest that most of the dissipated energy is released by restructuring the magnetic field, e.g. magnetic reconnection events.

During the impulsive phase of the flare, when the most powerful energization takes place, electrons must be accelerated to mean energies of about $\sim 25\mathrm{keV}$ at a rate of about $10^{36}$ electrons per second in order to sustain the observed intensity of the hard X-ray bursts. Taking the impulsive phase of a flare to last about $10\mathrm{s}$ and assuming an electron density of about $10^{10}\mathrm{cm}^{-3}$ (Moore & Fung 1972; Vaiana & Rosner 1978), the bulk energization must process a coronal volume of at least $10^{27}\mathrm{cm}^3$. Thus energization must affect a large fraction of the electron population in the flaring region.

In view of this background we want to briefly describe the processes which may be responsible for particle acceleration in solar flares. For a detailed review of possible acceleration processes in impulsive solar flares see e.g. Miller et al. (1997) and Cargill (1999).

1) *Shock Acceleration:* There are two types of shock acceleration. The one referred to as 'shock drift acceleration' involves the shock electric field that reflects and accelerates the particles moving along the shock surface. Since this mechanism is only effective when the shock normal approaches an angle of $90^\circ$ to the background magnetic field, either the gained energy or the particle flux is very limited. It seems to be unlikely that this mechanism is responsible for the large number of accelerated particles in solar flares. The second kind of shock acceleration is called 'diffusive shock acceleration'. In this process the particles cross the shock-front several times, interacting with scattering centers on both sides of the shock. In the rest frame of the shock these centers approach each other and the particles systematically gain energy. This kind of acceleration process requires a certain initial velocity in order to become effective. The ion velocity has to exceed the Alfvén speed $V_\mathrm{A} = \mathrm{B}_0/\sqrt{4\pi\rho}$ while the electrons must have velocities at least above $\sqrt{m_\mathrm{i}/m_\mathrm{e}}V_\mathrm{A}$. This has been called the 'injection problem'.

2) *Acceleration by parallel electric fields:* Direct acceleration by electric fields depend on its strength compared to the Dreicer field $E_D = (2\pi e^3 n_\mathrm{e} \ln\Lambda)/(k_\mathrm{B}T)$. If $E > E_\mathrm{D}$ most electrons and ions gain energy. If $E < E_\mathrm{D}$ only electrons in the high energy tail of the velocity distribution function will be accelerated. The limitation in both cases is the maintenance of overall neutrality of charge and pre-existing current in the acceleration region.

3) *MHD turbulence:* This acceleration mechanism occurs when particles interact many times with randomly moving MHD waves. Due to a slight overplus in head-on collisions the interaction results in an energy gain for the particle. As in the shock

*Send offprint requests to*: G. Paesold
*Correspondence to*: gpaesold@astro.phys.ethz.ch

acceleration model, the acceleration by MHD turbulence suffers from an 'injection problem': Thermal ions and electrons cannot resonate with MHD waves for typical solar pre-flare conditions.

A solution for this problem is the assumption of MHD turbulent cascades that channel the energy residing in the MHD turbulence to smaller scales and into the region where interaction with thermal particles is possible. A realization of this scenario is proposed in Miller (1991), Miller & Roberts (1995) and Miller (1997). An MHD turbulent cascade transfers the energy from large scale MHD waves to smaller scales where the energy may be absorbed by the particles. The mechanism that dissipates the wave energy into the particles is transit-time damping (Fisk 1976; Stix 1992). It is is basically a resonant Fermi acceleration of second order. Only particles in resonance with a low-amplitude MHD wave are affected. The resonance condition is the usual $l = 0$ (or Landau) resonance given by $\omega - k_\parallel v_\parallel \approx 0$. As the particles can only gain energy in the direction parallel to the background magnetic field, the temperature in parallel direction increases.

A preference for acceleration along the background magnetic field is a common feature of the acceleration models mentioned above. The velocity distribution thus becomes more and more anisotropic during acceleration. If energization in parallel direction is from a thermal level of some 0.1 keV to 20 keV or more but the perpendicular temperature remains constant, the anisotropy is substantial. The free energy residing in parallel direction may give rise to growth of plasma waves.

For $T_\parallel^\mathrm{e} > T_\perp^\mathrm{e}$ and high beta plasmas, Hollweg & Völk (1970) and Pilipp & Völk (1971) have proposed the Electron Firehose instability. This instability is an extension to higher frequencies of the (MHD) Firehose instability, originally mentioned by Parker (1958). While the Firehose instability is of a completely non-resonant nature, the Electron Firehose instability involves non-resonant electrons but resonant protons.

For large anisotropy of the electron distribution, the electrons become also resonant. This instability is described in Pilipp & Benz (1977) and is called the Resonant Electron Firehose instability.

Having been applied to a variety of problems, the Electron Firehose instability has not been considered to occur during electron acceleration in solar flares.

Here we investigate the threshold for growth of plasma modes resulting from acceleration and infer a prediction for the evolution of the distribution function in velocity space with respect to conditions expected to occur in solar flares.

We assume that no significant instability of Langmuir waves occurs. This is suggested by the following argument: If a large fraction of the available energy normally did go into Langmuir waves, we would expect always a radio signature orders of magnitude higher than ever observed during the impulsive phase (Benz & Smith 1987).

Sect. 2 describes the techniques used to solve the dispersion equations. In the following section the results obtained are shown and the thresholds of the instability are presented. In Sect. 4 we discuss the effect on the acceleration of electrons and conclude this work.

## 2. Method

Consider electromagnetic transverse waves of the form $\exp(ikx - i\omega t)$ propagating in the direction of the background magnetic field in an electron-proton plasma. The plasma dispersion equation can then be written as

$$\det\left((\mathbf{1}k^2 - \boldsymbol{k}\boldsymbol{k})\frac{c^2}{\omega^2} - \boldsymbol{\epsilon}(\omega,\boldsymbol{k})\right) = 0, \tag{1}$$

where, according to linearized kinetic theory, the dielectric tensor $\boldsymbol{\epsilon}(\omega,\boldsymbol{k})$ is given by

$$\boldsymbol{\epsilon}(\omega,\boldsymbol{k}) = \mathbf{1} - \frac{\omega_\mathrm{p}^2}{\omega^2}\left\{\mathbf{1} - \sum_j \sum_{n=-\infty}^{\infty} \int \boldsymbol{v}\prod \times \frac{\frac{n\Omega_j}{v_\perp}\frac{\partial}{\partial v_\perp} + k_\parallel \frac{\partial}{\partial v_\parallel}}{\omega - k_\parallel v_\parallel - n\Omega_j} f_j^0\right\}. \tag{2}$$

The gyrofrequency of the $j$th species is given by $\Omega_j = q_j B/(cm_j)$ and $\omega_\mathrm{p}$ denotes the plasma frequency defined as $\omega_\mathrm{p} = \sqrt{\sum_j \omega_{\mathrm{p}_j}^2} = \sqrt{\sum_j 4\pi n_j q_j^2/m_j}$. The tensor $\prod$ is given by the matrix

$$\prod = \begin{pmatrix} \left(\frac{n\Omega_j}{k_\perp}J_n\right)^2 & i\frac{n\Omega_j}{k_\perp}v_\perp J_n J_n' & \frac{n\Omega_j}{k_\perp}v_\parallel J_n^2 \\ -i\frac{n\Omega_j}{k_\perp}v_\perp J_n J_n' & (v_\perp J_n')^2 & -iv_\perp v_\parallel J_n J_n' \\ \frac{n\Omega_j}{k_\perp}v_\parallel J_n^2 & iv_\perp v_\parallel J_n J_n' & \left(v_\parallel J_n\right)^2 \end{pmatrix} \tag{3}$$

where the argument of the Bessel function $J_n$ is $k_\perp v_\perp/\Omega_j$. $f_j^0(v_\parallel, v_\perp)$ in Eq. (2) denotes the zero order distribution function in velocity space of the particle species $j$. In order to obtain full solutions of this equation, the computer code WHAMP (Rönnmark 1982) has been applied to the problem. The usage of this code has been facilitated by programming an interface for the programming language IDL. It is called IDLWhamp and provides the user with a comfortable tool to input parameters to the code and for management and visualization of the results.

According to the capability of the WHAMP code, the most general form of the particle distribution function $f_j^0(v_\parallel, v_\perp)$ for each species $j$ is given by

$$f_j^0(v_\parallel, v_\perp) = \frac{1}{\sqrt{2\pi}v_{j_\mathrm{th}}} \exp\left(-\left(\frac{v_\parallel}{2v_{j_\mathrm{th}}} - v_{dj}\right)^2\right) \times \left[\frac{\Delta_j}{\alpha_{1j}} \exp\left(-\frac{v_\perp^2}{2\alpha_{1j}v_{j_\mathrm{th}}^2}\right) + \frac{1-\Delta_j}{\alpha_{1j}-\alpha_{2j}} \times \left\{\exp\left(-\frac{v_\perp^2}{2\alpha_{1j}v_{j_\mathrm{th}}^2}\right) - \exp\left(-\frac{v_\perp^2}{2\alpha_{2j}v_{j_\mathrm{th}}^2}\right)\right\}\right]. \tag{4}$$

This is the original notation used in Rönnmark (1982) beside the choice of the thermal speed to be $v_{j_\mathrm{th}} = \sqrt{(k_\mathrm{B}T_j/m_j)}$. The $\alpha_{1j}$ parameter is the anisotropy $\alpha_{1j} = T_\perp^j/T_\parallel^j$ of the $j$-th

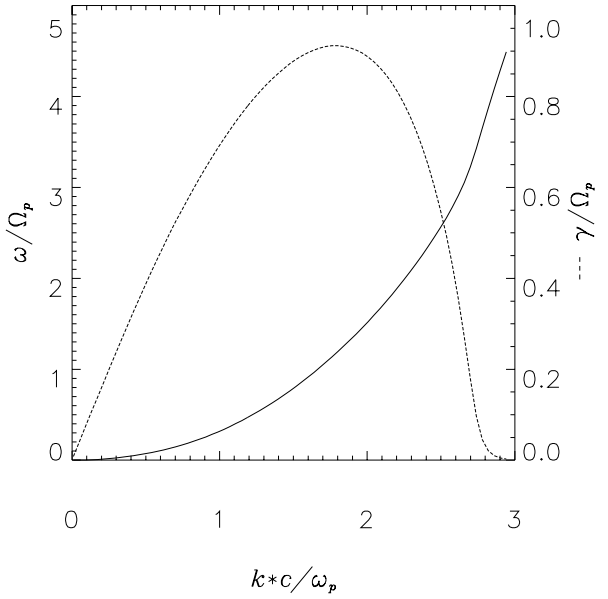


**Fig. 1.** A typical plot of the dispersion relation. The chosen parameters are $T_\perp^{\rm e} = T_\perp^{\rm p} = T_\parallel^{\rm p} = 10^7{\rm K}$, $\frac{T_\parallel}{T_\perp} = 20, n_{\rm e} = 5 \cdot 10^{10}{\rm cm}^{-3}, {\rm B}_0 = 100{\rm G}$. The real part of the frequency $\omega_{\rm r}$ and the growth rate $\gamma$ are normalized to the proton gyrofrequency $|\Omega_{\rm p}|$. The parallel wave vector is normalized to the proton inertial length. The whole branch is lefthand circularly polarized.

distribution function. $\Delta_j$ and $\alpha_{2j}$ define the depth and size of a possible loss-cone.

We assume that the electron velocity distribution function can be described by a bi-maxwellian with different temperatures in parallel and perpendicular direction with respect to the background magnetic field. Hence for our problem the parameters $\Delta_j$ and $\alpha_{2j}$ were set to unity in Eq. (4).

Taking into account the uncertainties in the acceleration region including a possible pre-heating mechanism altering the pre-flare plasma conditions, we do not want to restrict our work to the parameters of a particular scenario. According to Pallavicini et al. (1977) reasonable ranges in the acceleration region of an impulsive solar flare would be $\approx$ 100–500G for the background magnetic field, $\approx 10^9$–$10^{11}{\rm cm}^{-3}$ for the number density and $\approx 10^6$–$10^7$K for the temperature of electrons and protons.

## 3. Results

### *3.1. Electron Firehose instability*

The only mode exhibiting significant growth rates in our calculations is a lefthand circularly polarized wave which was identified to be the Electron Firehose instability. This mode evolves out of a stable righthand polarized whistler wave at small anisotropy. With increasing anisotropy, the frequency $\omega_{\rm r}$ is shifted so that, with the convention $\omega_{\rm r} > 0$, the mode becomes lefthand circularly polarized at $k||{\rm B}_0$ in the unstable regime, cf. Sect. 7 in Gary (1993). A typical dispersion relation is plotted in Fig. 1. By introducing the resonance factor

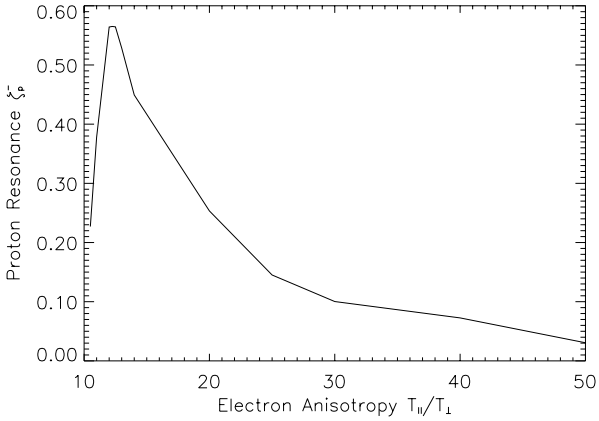


**Fig. 2.** Resonance factor $|\zeta_{\rm p}^-|$ of the protons versus the electron anisotropy $\frac{T_\parallel}{T_\perp}$ for the fastest growing modes. The larger $|\zeta_{\rm p}^-|$, the smaller is the fraction of protons in resonance.

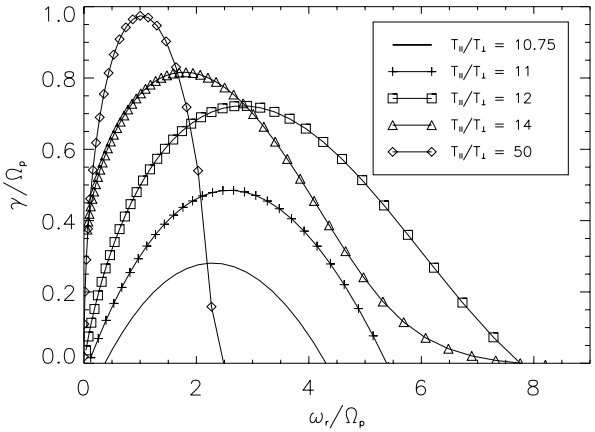


**Fig. 3.** The growth rate $\gamma$ versus the real part of the frequency $\omega_{\rm r}$, both normalized to the proton gyrofrequency, for different anisotropies $\frac{T_\parallel}{T_\perp}$. The values of the other plasma parameters are the same as in Fig. 1.

$$\zeta_j^\pm \equiv \frac{\omega_{\rm r} \pm \Omega_j}{\sqrt{2}|k_\parallel| v_{j_{\rm th}}}, \tag{5}$$

the values for the protons and electrons are found to be $|\zeta_{\rm p}^-| \sim 1$ and $|\zeta_{\rm e}^-| \gg 1$, demonstrating resonance for the protons and non-resonance for the electrons.

According to Hollweg & Völk (1970) there are also right hand circularly polarized modes, which can become unstable for this extension of the Firehose instability. These modes have been found, but the growth rates are smaller than the growth rates of the lefthand polarized modes described above.

As the instability first appears, the phase velocities of the resonant waves are near the peak of the proton distribution. Fig. 2 displays a plot of the proton resonance factor (5) for the fastest growing modes versus electron anisotropy. With increasing anisotropy less protons are resonant and the resonance factor increases. The change in the fraction of resonant protons is mirrored in the excited frequency range. As depicted in Fig. 3 the unstable frequency range grows to a maximum value at an anisotropy of about $\frac{T_\parallel}{T_\perp} \sim 12$, coinciding with the maximum

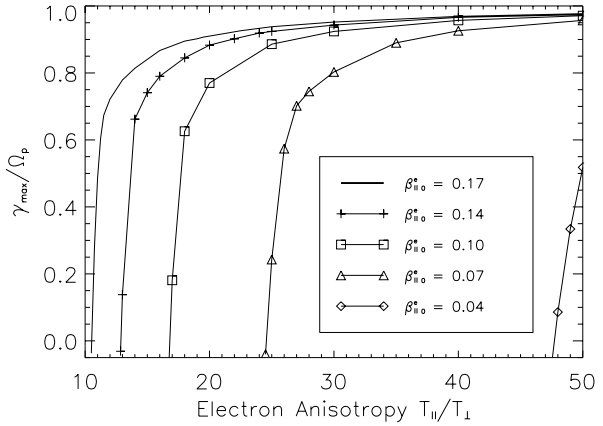


**Fig. 4.** The maximum growth rate $\gamma_{\max}$ normalized to the proton gyrofrequency $|\Omega_\mathrm{p}|$ versus the anisotropy $T_\parallel^\mathrm{e}/T_\perp^\mathrm{e}$ of the electrons; $T_\perp^\mathrm{p} = T_\parallel^\mathrm{p}$, $T_\perp^\mathrm{e} = T_\perp^\mathrm{p}$. The appropriate frequency is always of the order of $|\Omega_\mathrm{p}|$.

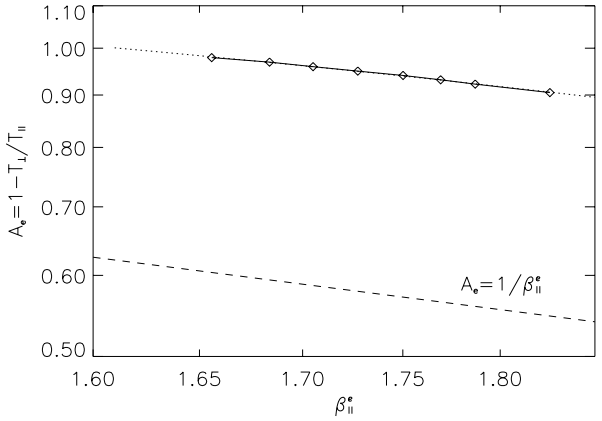


**Fig. 5.** Threshold for the Electron Firehose instability in anisotropy factor vs. parallel electron beta. The scaling of both axes is logarithmic. The dashed curve shows the instability limit according to Eq. (8). The dotted line represents a fit to the numerically obtained values which are depicted by diamonds. The areas above the respective lines are the unstable regions.

value of the resonance factor at $|\zeta_\mathrm{p}^-| \sim 0.57$ of the protons (cf. Fig. 2). As the resonance factor decreases again, the excited frequency range becomes narrow around $\omega_r/|\Omega_\mathrm{p}| \sim 1$. This narrow range is in itself evidence for the resonant character of the instability.

### *3.2. Instability threshold*

In this section we present the calculated threshold for linear growth of L-mode waves excited by the Electron Firehose instability.

The initial plasma is assumed to be maxwellian with temperatures $T_{\perp 0} = T_{\parallel 0} = T_0$ perpendicular and parallel to the background magnetic field for both plasma species, the electrons and the protons. Taking into account an acceleration mechanism for the electrons acting only in parallel direction, the perpendicular temperature remains constant throughout the whole acceleration process, i.e. $T_\perp^\mathrm{e} = T_{\perp 0}^\mathrm{e}$. In order to investigate the condition of the pre-flare plasma for the Electron Firehose instability to occur during the acceleration process, the initial plasma parameters have to be connected to the actual plasma parameters during the acceleration. With the assumptions above, this can be done by defining an initial parallel plasma beta, $\beta_{\parallel 0}^\mathrm{e}$, via the perpendicular plasma beta

$$\beta_{\parallel 0}^\mathrm{e} \equiv \beta_\perp^\mathrm{e} = \frac{8\pi n_\mathrm{e} k_\mathrm{B} T_\perp^\mathrm{e}}{{\mathrm{B}_0}^2}, \tag{6}$$

and the usual parallel plasma beta by

$$\beta_\parallel^\mathrm{e} \equiv \frac{8\pi n_\mathrm{e} k_\mathrm{B} T_\parallel^\mathrm{e}}{{\mathrm{B}_0}^2} = \beta_{\parallel 0}^\mathrm{e} \cdot \frac{T_\parallel^\mathrm{e}}{T_\perp^\mathrm{e}}, \tag{7}$$

where the connection between these two quantities is given by the temperature anisotropy $T_\parallel^\mathrm{e}/T_\perp^\mathrm{e}$.

According to Hollweg & Völk (1970) the instability criterion for the Electron Firehose instability may be approximated by

$$1 - \beta_\parallel^\mathrm{e} A_\mathrm{e} < 0, \tag{8}$$

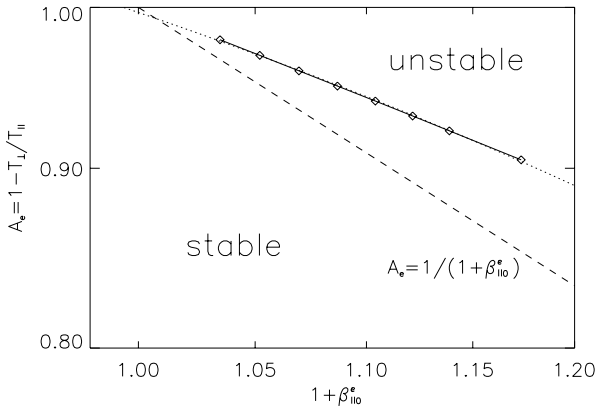


**Fig. 6.** The same plot as Fig. 5 but this time $A_\mathrm{e}$ has been plotted vs. the initial electron beta. Again, as in Fig. 5, the dashed curve shows the instability limit according to Eq. (8) and the dotted line represents a fit to the numerically obtained values.

where the anisotropy factor is defined by $A_\mathrm{e} = 1 - T_\perp^\mathrm{e}/T_\parallel^\mathrm{e}$.

As one can see from inequality (8), the instability threshold does not depend directly on the parameters $n_\mathrm{e}$, $T_\parallel^\mathrm{e}$, $\mathrm{B}_0$, but only on the resulting $\beta_\parallel^\mathrm{e}$. This independence is also reproduced with the numerically obtained data. For our purpose, the plasma is therefore fully described by the plasma beta.

In Fig. 4 the function $\gamma_{\max}(T_\parallel^\mathrm{e}/T_\perp^\mathrm{e})$ is plotted for five different values of $\beta_{\parallel 0}^\mathrm{e}$. The maximum growth rate of the instability steeply raises at the threshold of the instability and flattens for larger anisotropies, where $\gamma_{\max}/|\Omega_\mathrm{p}|$ approaches unity.

From these results, the contour of zero growth rate in the $A_\mathrm{e} - \beta_\parallel^\mathrm{e}$ plane has been derived (cf. Fig. 5). The discrepancy between the analytically derived relation (8) and the numerically obtained values is due to the approximation used in Hollweg & Völk (1970).

According to inequality (8), instability cannot occur for a parallel beta smaller than unity. Due to the deviations of the

approximation mentioned above, this limit is shifted to a value of $\sim 1.6$ (cf. Fig. 5).

In order to investigate the necessary properties of the pre-flare plasma for the Electron Firehose instability to occur, it is the initial plasma beta that is of interest. Fig. 6 depicts the same plot as Fig. 5 but this time the anisotropy factor $A_\mathrm{e}$ has been plotted versus the initial plasma beta $\beta^\mathrm{e}_{\parallel 0}$. The dotted line in both figures represents a fit to the numerically obtained values and is an extrapolation to a broader range of beta values. The negative $\beta^\mathrm{e}_{\parallel 0}$ at the $A_\mathrm{e} \to 1$ limit is an artifact of this extrapolation.

The values of the initial plasma beta for the Electron Firehose instability to occur at considerable values of $T^\mathrm{e}_\parallel / T^\mathrm{e}_\perp$ are well within the range of usually assumed pre-flare plasma parameters. For example, an initial plasma beta of $\beta^\mathrm{e}_{\parallel 0} \approx 0.05$ can be realized by assuming pre-flare plasma parameters of $n_\mathrm{e} = 5 \cdot 10^{10}\mathrm{cm}^{-3}$, $T^\mathrm{e}_0 = 3 \cdot 10^6\, K$ and $\mathrm{B}_0 = 100\mathrm{G}$. This plasma becomes unstable at an anisotropy of $T_\parallel / T_\perp \approx 32$.

According to the acceleration model via transit-time damping, this is a reasonable value for the anisotropy to occur during the acceleration process (Lenters & Miller 1998).

### *3.3. Influence of anisotropic protons*

If we assume the protons to be heated by the same or a similar mechanism, it is to be expected that they will grow anisotropic in the same way the electrons do. Hence, we also have investigated the influence of anisotropic protons and briefly discuss the effect of an additional proton anisotropy on the instability.

Consider a plasma with anisotropic electrons and isotropic protons that is already unstable to the Electron Firehose instability. When the protons are anisotropized by increasing the temperature in parallel direction, more and more become resonant to the L-waves, non-resonantly excited by the electrons. As shown by Hollweg & Völk (1970), the protons are damping these waves. Hence, it is to be expected that the resulting growth rate of the L-waves decreases as the proton anisotropy is increased. This expectation has been verified by numerical calculation.

Moreover, the protons are heated by absorption of the excited waves at the expense of the electrons (Pilipp & Völk 1971). According to Kennel & Petschek (1966) this scatters the protons to higher perpendicular velocities and hence, destroys or inverts the parallel proton anisotropy. It inhibits the growth of the electron anisotropy and may complicate the acceleration to higher energies, but increases the bulk energy of the protons. The energy transfer from the electrons to the protons via the Electron Firehose instability could be responsible for the proton energization, which is a problem in the transit-time damping scenario (Miller 1998).

If the protons are anisotropic, there is an additional righthand polarized wave mode. This mode is the extension of the lefthand Electron Firehose mode to negative frequencies. According to Hollweg & Völk (1970) this mode has real frequencies mainly below the proton gyrofrequency and is in resonance with the protons. As the anisotropy of the electrons increases, this righthand polarized mode becomes less and less significant.

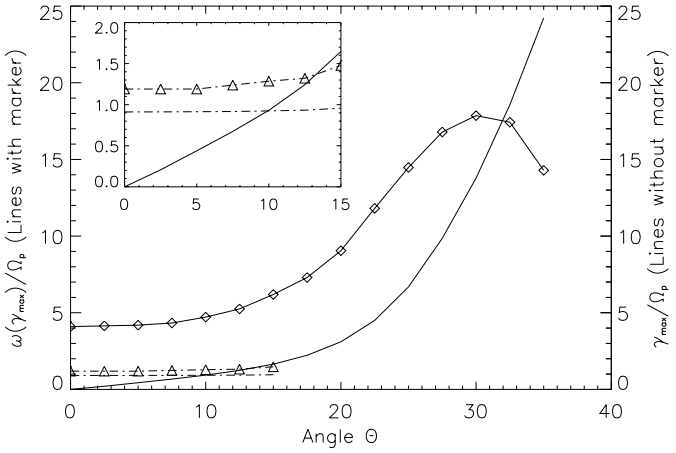


**Fig. 7.** Frequency and the according growth rates vs. the propagation angle $\Theta$ with respect to the background magnetic field. The dashed lines indicate the branch of the parallel Electron Firehose instability. The solid lines show the oblique mode that exhibit much faster growth than the Electron Firehose instability. The small plot is an enlargement of the region, where the crossing of the growth rates occurs. The plasma parameters are the same as in Fig. 1.

The proton cooling through the instability of the righthand mode competes with the heating by the lefthand mode and it is not yet clear what the net energization of the protons will be.

### *3.4. Oblique propagation: Preliminary results*

Sample calculations in oblique directions indicate an unstable branch of solutions that grows faster than the parallel Electron Firehose mode. This mode is stable at parallel propagation and is also lefthand circularly polarized. Fig. 7 depicts frequency and maximum growth rate versus the angle $\Theta$ of both modes. The dashed lines represent the branch, that is excited by the Electron Firehose instability at parallel propagation. At a propagation angle of about $10^\circ$ with respect to the background magnetic field, the growth rate of the oblique mode becomes larger than the growth rate of the parallel mode. Hence, the determining mode for instability thresholds is the oblique mode rather than the parallel Electron Firehose mode.

As calculations have shown, not only the growth rate of the oblique mode is larger than in the parallel case, but also the instability threshold may be lower with respect to anisotropy. Plasmas being stable with respect to the parallel mode exhibited instability to the oblique mode. Therefore, the thresholds for instability derived in the section above can be considered as upper boundaries.

Lefthand circularly polarized oblique modes seem to have never been considered in connection with the Electron Firehose instability. The further investigation of these modes is the subject of ongoing work.

## 4. Discussion and conclusion

Numerical solutions of the dispersion equation for lefthand circularly polarized electromagnetic waves, propagating parallel

to the background magnetic field, have shown that the Electron Firehose instability, usually considered as a 'high-beta plasma' instability, must be expected in coronal plasmas which are processed by an acceleration mechanism with a preference in parallel direction. The distribution function of the electrons in velocity space has been represented by a bi-maxwellian with temperatures $T_{\perp}^{\mathrm{e}}$ and $T_{\parallel}^{\mathrm{e}}$, perpendicular and parallel with respect to the background magnetic field. The protons have been assumed to be isotropic and in thermal equilibrium.

Considering the uncertainty in the pre-flare conditions, we have investigated instabilities in a broad range of plasma temperature $T$, density $n$ and background magnetic field $\mathrm{B}_0$. For these plasmas, it was found that the Electron Firehose instability occurs at anisotropies that must be expected for an acceleration mechanism acting predominantly in parallel direction and being capable of producing the observed electron bulk energization.

The unstable parallel modes that have been found are lefthand circularly polarized and non-resonantly excited by the electrons, but partially cyclotron resonant with the protons, which absorb the wave energy. Hence, energy is transferred from the electrons to the protons. Assuming the density and the magnetic field to be constant during the acceleration process, there is a limiting electron temperature in parallel direction that cannot be exceeded without loosing energy to the protons via the Electron Firehose instability. The Electron Firehose instability may thus inhibit the electron acceleration process and limit the reachable energies.

At angles $\Theta \neq 0$ with respect to the background magnetic field, an oblique mode has been found, that exhibits even larger growth rate than the parallel Electron Firehose instability. This mode is also lefthand circularly polarized. The properties of the oblique mode open new aspects on the Electron Firehose instability and its thresholds.

Taking anisotropic protons into account, the lefthand mode may extend to negative frequencies. They correspond to the righthand circularly polarized mode resonantly excited by the protons. Due to the cooling effect of this instability it is not yet clear to what the net energization of the electrons and the protons will amount. This topic will be the subject of future particle simulations.

*Acknowledgements.* The authors thank S. Peter Gary and James A. Miller for their helpful advice and Kjell Rönnmark for providing them with a copy of the KGI report describing the original WHAMP code. The authors also want to acknowledge Gérard Belmont and Laurence Rezeau who gave them free access to their improved version of the WHAMP code, which has become the mathematical core of IDLWhamp. This work was financially supported by the Swiss National Science Foundation (grant No. 20-53664.98).

## References

Benz A.O., Smith D.F., 1987, Solar Physics 107, 299
Cargill P., 1999, Solar Flares: Particle Acceleration Mechanisms. In: Priest E. (ed.) Encyclopedia of Astronomy and Astrophysics. Institute of Physics and Macmillan Publishing, in press
Fisk L.A., 1976, Journal of Geophysical Research 81, 4633
Gary S.P., 1993, Theory of Space Plasma Microinstabilities. Cambridge University Press
Hollweg J.V., Völk H.J., 1970, Journal of Geophysical Research 75/28, 5297
Kennel C.F., Petschek H.E., 1966, Journal of Geophysical Research 71/1, 1
Lenters G.T., Miller J.A., 1998, ApJ 493, 451
Miller J.A., 1991, ApJ 376, 342
Miller J.A., 1997, ApJ 491, 939
Miller J.A., 1998, Space Sci. Rev. 86, 79
Miller J.A., Cargill P.J., Emslie A.G., et al., 1997, Journal of Geophysical Research 102/A7, 14'631
Miller J.A., Roberts D.A., 1995, ApJ 452, 912
Moore R.L., Fung P.C.W., 1972, Solar Physics 23, 78
Pallavicini R., Serio S., Vaiana G.S., 1977, ApJ 216, 108
Parker E.N., 1958, Physical Review 109, 1874
Pilipp W., Benz A.O., 1977, A&A 56, 39
Pilipp W., Völk H.J., 1971, Journal of Plasma Physics 6, 1
Roennmark K., 1982, KGI Report, 179
Stix T.H., 1992, Waves in Plasmas. AIP, New York, 273
Vaiana G.S., Rosner R., 1978, ARA&A 16, 393